



**HAL**  
open science

## Electronic and magnetic properties of the multiferroic TbMn<sub>2</sub>O<sub>5</sub>

A. Endichi, Hamza Bouhani, H. Zaari, M. Balli, O. Mounkachi, A. El Kenz,  
A. Benyoussef, Stéphane Mangin

► **To cite this version:**

A. Endichi, Hamza Bouhani, H. Zaari, M. Balli, O. Mounkachi, et al.. Electronic and magnetic properties of the multiferroic TbMn<sub>2</sub>O<sub>5</sub>. Applied physics. A, Materials science & processing, 2020, 126, 10.1007/s00339-020-03585-4 . hal-02901659

**HAL Id: hal-02901659**

**<https://hal.univ-lorraine.fr/hal-02901659v1>**

Submitted on 17 Jul 2020

**HAL** is a multi-disciplinary open access archive for the deposit and dissemination of scientific research documents, whether they are published or not. The documents may come from teaching and research institutions in France or abroad, or from public or private research centers.

L'archive ouverte pluridisciplinaire **HAL**, est destinée au dépôt et à la diffusion de documents scientifiques de niveau recherche, publiés ou non, émanant des établissements d'enseignement et de recherche français ou étrangers, des laboratoires publics ou privés.

# Electronic and magnetic properties of the multiferroic TbMn<sub>2</sub>O<sub>5</sub>

**A. Endichi<sup>1,2,\*</sup>, H. Bouhani<sup>1,2</sup>, H. Zaari<sup>1</sup>, M. Balli<sup>3,4</sup>, O. Mounkachi<sup>1</sup>, A. El Kenz<sup>1</sup>, A. Benyoussef<sup>5,6</sup> and S. Mangin<sup>2</sup>**

<sup>1</sup>*LaMCSl, B.P. 1014, Faculty of Science-Mohammed V University, Rabat, Morocco*

<sup>2</sup>*Institut Jean Lamour, UMR CNRS 7198–Université de Lorraine–BP 70239, F-54506 Nancy, France*

<sup>3</sup>*LERMA, ECINE, International University of Rabat, Parc Technopolis, Rocade de Rabat-Salé, 11100, Morocco.*

<sup>4</sup>*Département de physique & Institut Quantique, Université de Sherbrooke, J1K 2R1 Québec, Canada*

<sup>5</sup>*Materials and Nanomaterials Centre, Moroccan Foundation for Advanced Science, Innovation and Research, MAScIR, Rabat, Morocco*

<sup>6</sup>*Hassan II Academy of Science and Technology, Rabat, Morocco*

## Abstract

Recently, a reversible and a giant rotating magneto-caloric effect has been pointed out in the multiferroic TbMn<sub>2</sub>O<sub>5</sub> single crystal, opening the way for new designs of low-temperature magnetic cooling. In this paper, we report a preliminary theoretical work with the aim of enlarging our understanding on the electronic, magnetic and accordingly magnetocaloric features of the TbMn<sub>2</sub>O<sub>5</sub> compound. Particularly, the TbMn<sub>2</sub>O<sub>5</sub> magnetic anisotropy is analyzed in terms of X-ray Magnetic Circular Dichroism (XMCD) and X-ray absorption spectroscopy (XAS) spectra.

**Keywords:** Multiferroic materials, Magnetoelectric effect, magnetic anisotropy, XAS, XMCD, DFT.

---

\*Corresponding author : [asmae.endi@gmail.com](mailto:asmae.endi@gmail.com)

## 1. Introduction:

The discovery of new multiferroic compounds exhibiting a strong magneto-electric coupling has aroused great interest since the beginning of the century, justified both by the fundamental issues involved and the prospects for technological applications [1]. The interest of these compounds lies in the coupling between orders, magnetic and electrical, with the possibility, from a static point of view, to manipulate the magnetization by applying an electric field [2]. The more recent discovery of magneto-electric excitations has opened up a new field investigation [3]. In multiferroics, these hybrid excitations, called electromagnons can be understood as magnons excited by the electrical component of a wave electromagnetic and are the signature in the dynamic regime of magneto-electric coupling [4, 5]. Understanding the mechanisms behind these new excitations is one of the recent challenges of condensed matter physics, and the possibility of modulating these excitations via a field electric and / or magnetic is also an avenue explored for future applications to be defined in the field of information transport, magnetic refrigeration and spintronic devices for example. These materials in which the magnetism and the ferroelectricity are coupled have been widely studied [6, 7, 8]. Studies on  $\text{RMn}_2\text{O}_5$  oxides have shown an important magneto-caloric effect (MEE) that is associated with a unique commensurate-incommensurate magnetic transition [1-9].

In this way, by using relatively low magnetic fields a highly reversible switching of electrical polarization was reported in  $\text{TbMn}_2\text{O}_5$  [10]. On the other hand, it was recently shown that the same compound unveils a giant and reversible rotating magnetocaloric effect (RMCE). Habitually, this compound exhibits an insulating behavior. Its crystalline structure consists of edge-shared  $\text{Mn}^{4+}\text{O}_6$  octahedra arranged along the *c*-axis and linked by pairs of  $\text{Mn}^{3+}\text{O}_5$  pyramids [11, 12, 13, 14]. The multiferroic  $\text{TbMn}_2\text{O}_5$  material is characterized also by different exchange interactions involving  $\text{Mn}^{4+}$ ,  $\text{Mn}^{3+}$  and rare earth  $\text{R}^{3+}$  ions sublattices, leading to a complex magnetism character. As a result,  $\text{TbMn}_2\text{O}_5$  reveals various magnetic and electric phase transitions [15, 16]. At  $T_N = 43$  K, it shows an incommensurate antiferromagnetic (ICM) state with a propagation vector  $\mathbf{k}$  (0.50, 0, 0.30) that transforms into a commensurate antiferromagnetic (CM) phase at  $T_{\text{CM}} = 33$  K with  $\mathbf{k} = (0.5, 0, 0.25)$ , while a ferroelectric order takes place at  $T_{\text{FE}} = 38$  K [15].

Recently, it has been demonstrated that a large thermal effect can be simply produced by rotating the  $\text{TbMn}_2\text{O}_5$  single crystal within the *ac*-plane in relatively low constant magnetic fields rather than using the conventional magnetization-demagnetization method [1]. Under a constant magnetic field of 2T, the resulting maximum entropy change from the rotation motion is more than 6 J/kg K, while

the associated adiabatic temperature change is found to exceed 8K. Such a large RMCE was attributed to different factors such as strong magnetocrystalline anisotropy, low specific heat as well as the enhancement of the magnetization under magnetic fields lower than 3T. In this work, the first principles calculations (DFT) are used to investigate the electronic and magnetic properties of TbMn<sub>2</sub>O<sub>5</sub>, we aim at opening the way for the understanding of the physics behind the RMCE in TbMn<sub>2</sub>O<sub>5</sub> single crystals and the promising RMn<sub>2</sub>O<sub>5</sub> family of multiferroics [16].

## 2. Computational method

The TbMn<sub>2</sub>O<sub>5</sub> compound crystallizes in an orthorhombic symmetry with Pbam space group (number 55). Its lattice parameters are given by:  $a = 7.2643 \text{ \AA}$ ,  $b = 8.4768 \text{ \AA}$  and,  $c = 5.6700 \text{ \AA}$  [17]. The electronic and magnetic properties of TbMn<sub>2</sub>O<sub>5</sub> have been studied using ab-initio calculations with full-potential linearized augmented plane-wave (FP-LAPW) [18] involving the gradient generalized approximation GGA [19], GGA+U and spin-orbit coupling.

Conventional approaches such as the local density approximation (LDA) [20], or that of generalized gradients (GGA) [21], used in density functional theory (DFT), are standards and widely used as an approach to describe the ground state of a large number of insulating, semiconductor and metallic systems. However, it seems to us that they are insufficient to obtain a satisfactory qualitative description of the structure electronics and magnetic properties of correlated systems, so it is necessary to go beyond the DFT to properly treat strong electronic correlations. Several corrections have been developed to provide solutions to this DFT deficiency.

Among those which have been applied, we find the GGA+U method [22, 23], where "U" is the Hubbard parameter which designates the intra-atomic Coulomb interaction applying to localized orbitals (In general d or f) to correct errors in the DFT.

In TbMn<sub>2</sub>O<sub>5</sub>, U is equal to 8eV for Tb and 4eV for Mn while J is assumed to be zero for both atoms [19]. The total and partial electron densities are calculated at equilibrium state. The self-consistent calculations are considered to converge with a convergence criterion fixed by a variation of the sixth decimal place in the electronic charge density and with 7x6x9 Monkhorst-Pack mesh implemented in the code WIEN2k [24]. In this work, calculations are performed on the Pbam orthorhombic structure of TbMn<sub>2</sub>O<sub>5</sub> reported in Figure 1 using the reported crystallographic parameters in ref [17].

To determine the magnetic anisotropy, we have utilized DIPAN program implemented in WIEN2K code [18] that calculates the magnetic dipolar hyperfine field and the dipolar magneto-crystalline anisotropy.

It is theoretically possible to measure the XMCD signal of any compound having at least one paramagnetic moment and for which the spin-orbit coupling is not zero. The analysis of XMCD spectra allows, with the "sum rules", to go back to the moment of spin and orbit of the studied element TbMn<sub>2</sub>O<sub>5</sub>. It is necessary for that, firstly, to have the absorption field in zero field and calculate it's integral, secondly, to make the difference of the two absorptions obtained for the two polarizations, it is the signal XMCD [24]. This signal is employed to estimate the value of the spin and orbital moments in TbMn<sub>2</sub>O<sub>5</sub> compound.

Also, the XMCD spin moment sum rule to the M<sub>4,5</sub> edges of Tb is used for the calculation of orbital and spin moments. Considering the transition 3d (c = 2) into 4f final states (l=3) with the number of holes n = 4l+2-n<sub>4f</sub>, the following equations are obtained [25]:

$$m_L = (\mu_b / \hbar) \langle L_z \rangle = -2 \left( \frac{\int_{M_4+M_5} d\omega(\mu^+ - \mu^-)}{\int_{M_4+M_5} d\omega(\mu^+ + \mu^-)} \right) * (14 - n_{4f}) \quad (1)$$

$$m_S = (\mu_b / \hbar) \langle S_z \rangle = \left( \frac{7 \int_{M_5} d\omega(\mu^+ - \mu^-) - 6 \int_{M_4} d\omega(\mu^+ - \mu^-)}{\int_{M_4+M_5} d\omega(\mu^+ + \mu^-)} * (14 - n_{4f}) \right) \left( 1 + 10 \frac{\langle T_z \rangle}{\langle S_z \rangle} \right)^{-1} \quad (2)$$

Where the  $S_z$  and  $L_z$  are the spin and orbital moment of Tb atoms, respectively.

### 3. Results and discussion

The compound TbMn<sub>2</sub>O<sub>5</sub> has an orthorhombic structure consisting of octahedra of Mn<sup>4+</sup>O<sub>6</sub> and bipyramids of Mn<sup>3+</sup>O<sub>5</sub> linked by their edges and their corners. This structure is illustrated in FIG. 1. Perfect knowledge of the magnetic orders of the Mn<sup>3+</sup> and Mn<sup>4+</sup> ions is essential for a good understanding of the multiferroic character of the compound TbMn<sub>2</sub>O<sub>5</sub>.

This material has several magnetic transitions. Below 10 K, the magnetic order of the Tb ion spins appears and adopts an antiferromagnetic order. Given the complexity of these magnetic orders, we will simplify the diagram of these configurations by looking at the ab plane, in which the ion spins Mn are almost confined.

The front view of the ab plane shows that the crystal structure of TbMn<sub>2</sub>O<sub>5</sub> is formed by two loops of manganese ions. Each loop consists of a chain of manganese ions Mn<sup>4+</sup> -- Mn<sup>3+</sup> -- Mn<sup>3+</sup> -- Mn<sup>4+</sup> -- Mn<sup>3+</sup> which forms a pentagonal loop. The two loops share two neighboring Mn<sup>3+</sup>O<sub>5</sub> pyramids. However, if an antiferromagnetic coupling between two neighboring spins is established, it should favor an antiparallel arrangement along the entire chain. However, this is not the case. Indeed,

geometrically, one cannot form an antiferromagnetic order along a loop formed by five manganese ions. This creates a frustrated magnetic structure which gives rise to more complex magnetic orders.

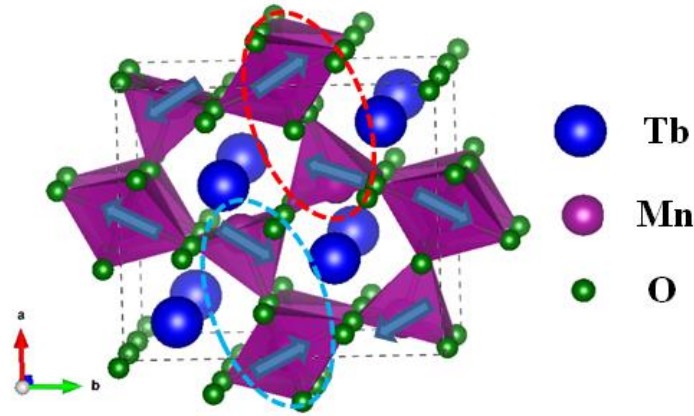


**Figure 1: Orthorhombic structure of  $\text{TbMn}_2\text{O}_5$ , the blue arrows indicate the magnetic structure of manganese ions.**

Figure 1 shows the magnetic configuration of  $\text{TbMn}_2\text{O}_5$  in the commensurate antiferromagnetic phase, the spins of which are ordered antiparallelically along the zigzag chain along the b axis. The neighboring pairs  $\text{Mn}^{3+} - \text{Mn}^{4+}$  are alternately coupled in a quasi-ferromagnetic and quasi-antiferromagnetic manner along the axis a (ellipses in red and blue dotted lines).

### 3.1 Electronic properties

As we had discussed previously,  $\text{TbMn}_2\text{O}_5$  crystallizes in an orthorhombic structure of space group  $Pb_{21}m$ , The manganese in this structure have two valences,  $\text{Mn}^{3+}$  and  $\text{Mn}^{4+}$ , corresponding to two crystallographic sites, The cations  $\text{Mn}^{4+}$  have an octahedral environment of six oxygen (Fig 2). The octahedra are joined together by a ridge and form continuous chains along the c axis. The  $\text{Mn}^{3+}$  environment has pyramids with a square base of five oxygen.

They are organized in dimers in which the two pyramids share an edge. Octahedra and bipyramids constitute the elementary building bricks. Along the c axis, there is an alternation of planes of pyramids  $\text{Mn}^{3+}\text{O}_5$ , octahedra  $\text{Mn}^{4+}\text{O}_6$  and rare earth  $\text{Tb}^{3+}$ .

The crystallographic sites and the coordinates of the ions in the mesh are given in the following table:

**Table 1: Atoms positions in  $\text{TbMn}_2\text{O}_5$**

Ion	Name	Position
Tb <sup>3+</sup>	Tb	(x, y, 0)
Mn <sup>3+</sup>	Mn1	(0, 0.5, z)
Mn <sup>4+</sup>	Mn2	(x, y, 0.5)
O	O1	(0, 0, z)
O	O2	(x, y, 0)
O	O3	(x, y, 0.5)
O	O4	(x, y, z)

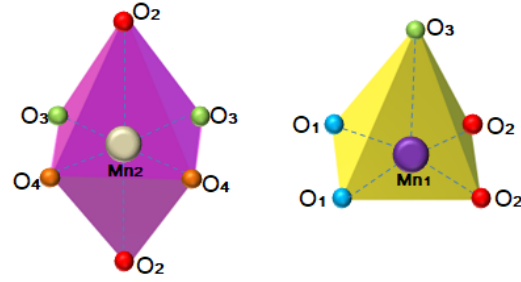


**Figure 2: Basic structural units of distorted Mn1O<sub>5</sub> octahedra and Mn2O<sub>6</sub> square pyramid**

In order to explain the impact of electronic structure on the magnetic properties, we have calculated the total and partial densities of states (PDOS) of TbMn<sub>2</sub>O<sub>5</sub> with GGA and GGA+U approximations as they are displayed in Fig.3(a) and Fig.3(b). The lower valence bands situated in the range (-7.0 eV) to (-5.0 eV) is due to the Tb-f states. The main contribution to the magnetism comes from 4f states of Tb atoms.

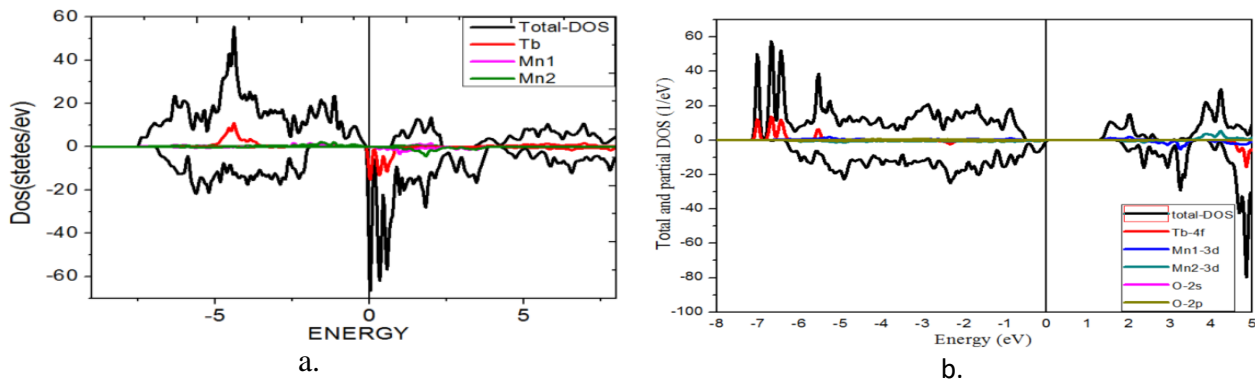


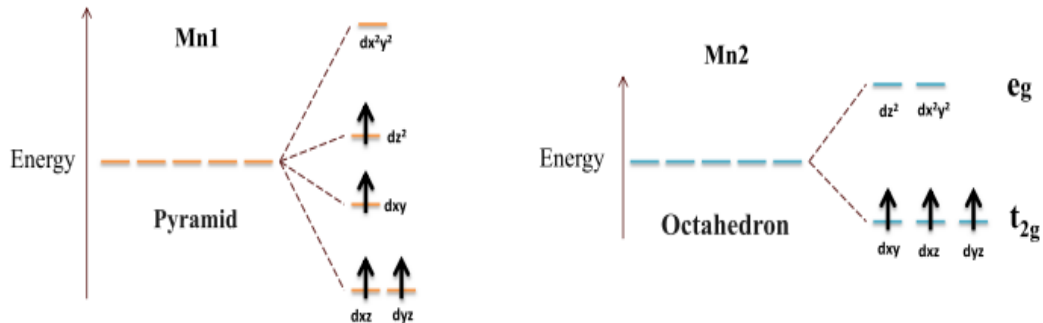
**Figure 3: (a) Total density of states for TbMn<sub>2</sub>O<sub>5</sub> with the GGA approximation. (b) Total and partial density of states for TbMn<sub>2</sub>O<sub>5</sub> with the GGA+U approximation.**

The detail of the structure strongly depends on the nature of Terbium. It is not only the order of moments of Tb<sup>3+</sup> which differs from one compound to another of the same family, but also the order of moments of Mn can also be influenced [26, 27]. This indicates the role of Tb in the magnetic ordering of manganese ions. Indeed, with its strong spin-orbit coupling, the Tb<sup>3+</sup> ion has a strong anisotropy. Since that of manganese ions is much weaker, it is expected that the magnetic order in TbMn<sub>2</sub>O<sub>5</sub> will depend on the anisotropy of Terbium.

The filling of the d orbitals in a pyramidal environment with a square base and in an octahedral environment is done by respecting Hund's rule (the energy of repulsion is minimized by adopting a maximum spin state).

The environment of the terbium, having 8 first neighbors, and the nature of the 4f orbitals being more complex, the estimation of the degeneration and the filling of these orbitals requires more detailed

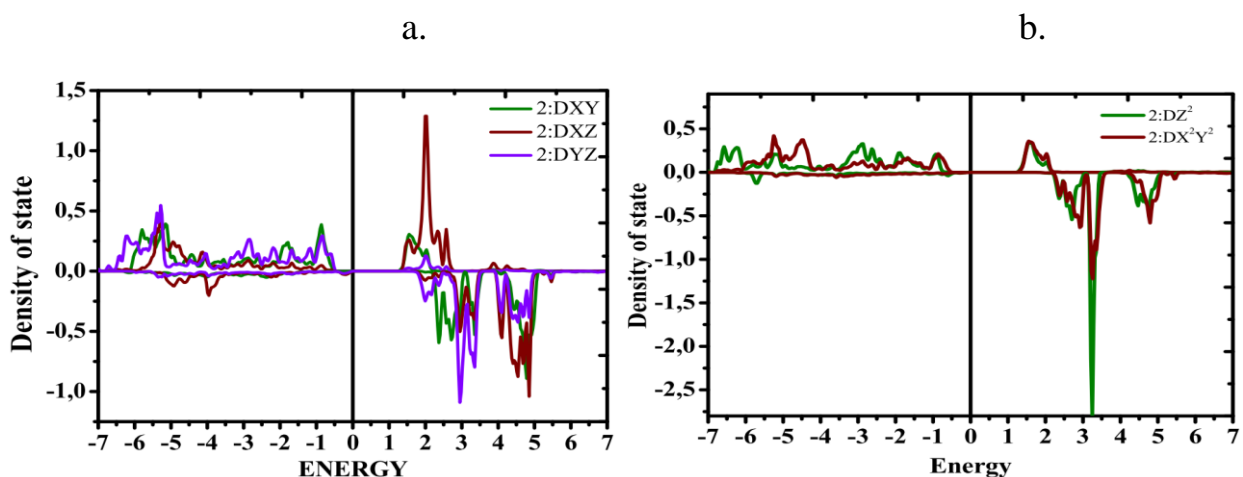
calculations based on a precise crystallographic structure. The nature of the occupied 3d and 4f orbitals and the fine crystallographic structure are essential parameters for the calculation of the exchange integrals.



**Figure 4: Energy levels and filling of 3d manganese orbitals in a pyramidal (left) and octahedral (right) environment.**

The Pbam symmetry of  $\text{TbMn}_2\text{O}_5$  allows a position freedom of  $\text{Mn}^{3+}$  ions along the pyramid axis. Such motion alters the Mn-O bonds, and thus the hybridization between the manganese 3d and oxygen 2p states. It is worth noting that the U value is taken from ref [28].

The density of states for Mn1 show that the  $t_{2g}$  level gives rise to two levels: a level which remains stable with a pure metallic character dxy and a level formed by the two hybrid molecular orbitals with a metallic character dxz and dyz, this level is a little destabilized because of the decrease in the binding character metal ligand. The level eg generates an undisturbed level formed predominantly of  $dx^2-y^2$ , and a  $dz^2$  level which is stabilized (see Fig 4 and 5).



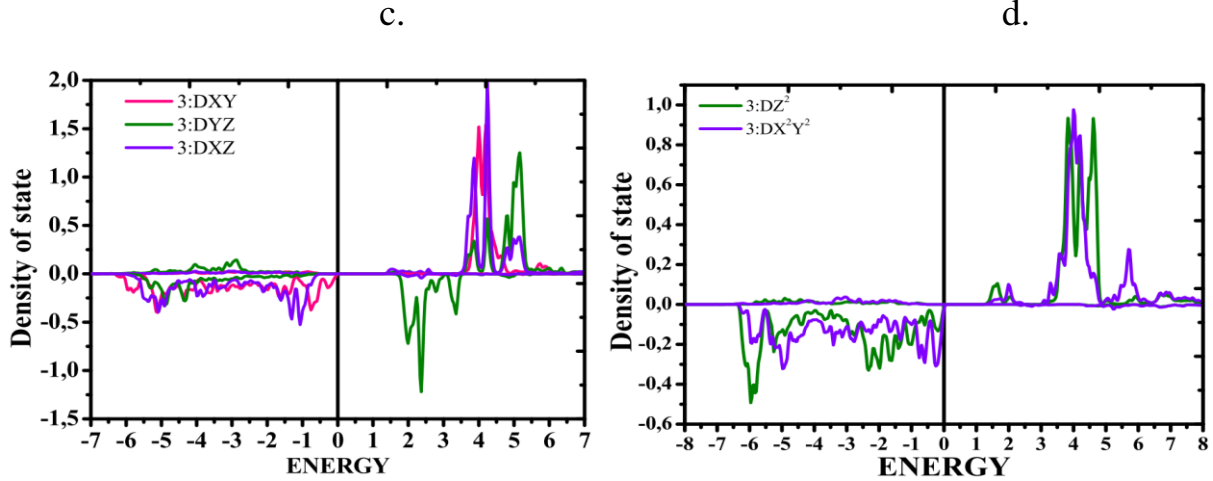


**Figure 5:** The density of state as a function of energy (eV), of Mn1 (number 2) and Mn2 (number 3) atoms, (a) dxy, dxz and dyz states, (b) dz<sup>2</sup> and dx<sup>2</sup>y<sup>2</sup> states for Mn1 atoms, and (c) dxy, dxz and dyz states, (d) dz<sup>2</sup> and dx<sup>2</sup>y<sup>2</sup> states for Mn2 atoms.

### 3.2 Magnetic properties

In order to well understand the magnetic interactions in the TbMn<sub>2</sub>O<sub>5</sub> compound, we have calculated the values of Tb and Mn spins and their orbital magnetic moments [29]. The sign of the XMCD signal and that of its integral give the relative orientation of the magnetic moments between them and with respect to the applied external field.

For the total magnetic moment given in The Self-Consistent Field (SCF) calculation, it is difficult to distinguish between the contributions from the spins and orbitals since it is equivalent to the difference between up and down spin densities of state.

For these reasons XMCD can gives more details about the value of spin-orbit coupling and calculate separately the spin and orbital moments. The absorption and dichroic spectra XAS and XMCD of TbMn<sub>2</sub>O<sub>5</sub> are shown in Fig.6(a) and Fig.6(b). At the M edge, the absorption spectrum presents a peak situated at 1208.0 eV. At the L<sub>2</sub> edge, the spectrum presents one contribution at 1244.5 eV. The integral of XMCD and XAS allows the calculation of orbital  $m_{orb}$  and spin  $m_s$  moments.

**a.**

**b.**

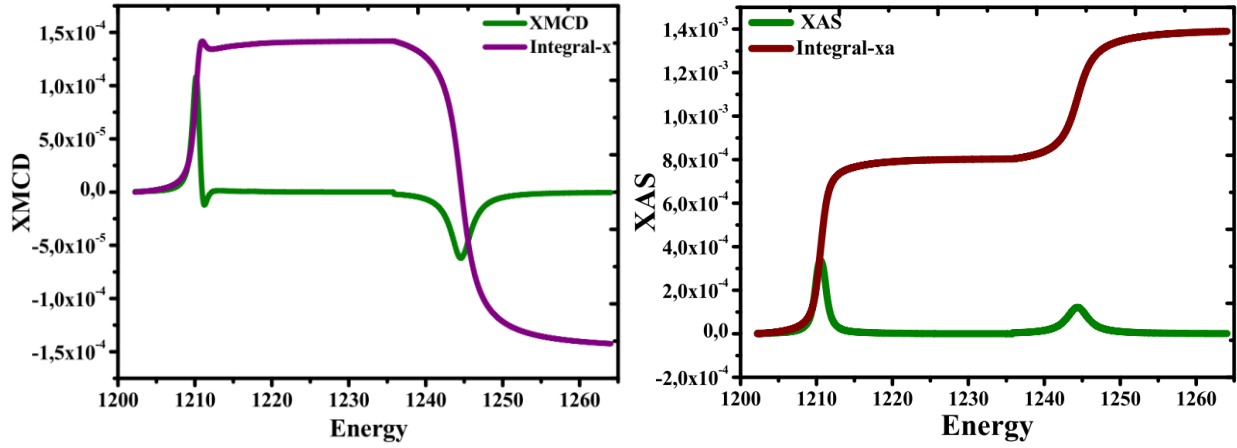


**Figure 6:** (a) X-ray magnetic circular dichroism (XMCD) spectra of  $\text{TbMn}_2\text{O}_5$ . (b) X-ray absorption spectroscopy (XAS) spectra of  $\text{TbMn}_2\text{O}_5$ .

The number of 4f-electrons ( $3d$ ) is calculated by integrating the 4f projected ( $3d$ ) density of states inside each atomic sphere. According to the relations (1) and (2) and using GGA approximation, the values of  $m_{\text{orb}}$  and  $m_s$  are given in Table 2 for both Tb and Mn atoms. These values indicate on the strong contribution of Tb ions to the total magnetic moment [30]. On other hand, the obtained moment for Tb compares well with that experimentally reported in Refs. [1] and [31].

**Table 2:** The orbital and spin moments of Tb, Mn1 and Mn2 atoms for  $\text{TbMn}_2\text{O}_5$ .

	XMCD			Experimental
	Tb	Mn1	Mn2	Tb
Spin moment ( $\mu\text{B}$ )	6.9	-2.01	1.44	-
Orbital moment ( $\mu\text{B}$ )	1.69	-0.15	0.06	-
Total moment ( $\mu\text{B}$ )	8.59	-	-	9.34[32]

In  $\text{TbMn}_2\text{O}_5$  compound, giant magnetocrystalline anisotropy is remarked where the magnetization tends to orient preferentially along the a-axis [1, 31] (along the b-axis for  $\text{HoMn}_2\text{O}_5$  [33]). As mentioned before, the DFT calculations using xdiplan program enabled us to determine the minimal energy corresponding to the easy-axis of magnetization. Thus, the magnetic anisotropy is defined as:

$$\Delta E = E(\text{easy axis}) - E(\text{hard axis}).$$

The spin-orbit term is included to observe the change in density of states. For 4f states and 3d states, it is known that there is a competition between the spin-orbit effect and the crystal field. The latter is usually strong in the case of 3d states (transition metals). Also, the rare earth elements require a spin-orbit calculation. So, it is highly important to see the charge distribution in 3d and 4f states in the case of spin orbit coupling (SOC). To understand the anisotropy shown by  $\text{TbMn}_2\text{O}_5$ , we calculated the

energy of the compound following each axis using DIPAN package implemented in WIEN2k program. The calculation consists to compute the total energy for different axes to find the minimal one. For  $\text{TbMn}_2\text{O}_5$ , the lower value corresponds to the a-axis, confirming early reported experimental works [1, 34].

The Hubbard U potential makes it possible to localized f and d states or the electrons which are delocalized.

The localization of these bands which are responsible for the magnetisms makes it possible to better calculate the magnetic moment and the most stable magnetic phase, as well as the spin orientation of each electron which gives access to the orientation of the magnetization in the compound. In fact we obtain the most probable value of magnetic anisotropy energy (MAE).

**Table 3: Magnetic anisotropy of  $\text{TbMn}_2\text{O}_5$  using GGA and GGA+U**

Direction	$E_{\text{anj}}(\text{J/m}^3)$	
	GGA	GGA+U
[001]	$-0,8625.10^3$	$-0,7853.10^4$
[100]	$-0,2985.10^4$	$0,1474.10^5$
[010]	$-0,7825.10^3$	$-0,6890.10^4$
[110]	$-0,1311.10^4$	$0.2292.10^4$
[101]	$-0,4524.10^3$	$0,6133.10^4$
[011]	$-0,6167.10^3$	$-0,7190.10^4$
[111]	$-0,2786.10^3$	$0.19058.10^3$

It seems from the table 3 that the calculations without applying the potential U give the easy magnetization axis on the a axis while the correction U gave a minimum energy on the [011] axis or the (001) plane.

It should be noted that the magnetic anisotropy is given by the Wien2k code using the Dipan package, which just gives an anisotropy contribution, in particular it is the anisotropy created by the network. For the correction U, the easy magnetization axis is located between the z axis and the yz plane, which confirms the non-collinearity of the spins of magnetic atoms [35].

#### 4. Conclusion:

In summary, our preliminary calculations using the density functional theory study of  $\text{TbMn}_2\text{O}_5$  unveil that it is possible to determine some key parameters such as magnetic moments and electronic structures that are of great interest for the investigation of its entropic behavior (MCE). Particularly, the obtained magnetic moments as well as the anisotropic energies are in fair agreement with previous experimental reports. However, the main challenge remains the simulation of some important magnetothermal parameters of  $\text{TbMn}_2\text{O}_5$  such as specific heat, entropy and adiabatic temperature changes. This point is currently under investigation in our group and any relevant results will be published in a forthcoming publication.

### **Acknowledgments:**

This work was supported by **PHC Toubkal/17/49- 36812NJ** project, and by the MESRSFC (Ministere de l'Enseignement Supérieur, de la Recherche Scientifique et de la formation des cadres) in the framework of the national program PPR under contract no. PPR/2015/57.

### **References:**

- [1] M. Balli, S. Jandl, P. Fournier, and D. Z. Dimitrov, *Appl. Phys. Lett* 108, 102401 (2016).
- [2] H. Katsura, N. Nagaosa, and A. V. Balatsky, *Phys. Rev. Lett.* 95, 057205 (2005).
- [3] M. Fiebig, *J. Phys. D: Appl. Phys.* 38, R123 (2005).
- [4] Graeme Eoin Johnstone, “Neutron and X-ray Scattering Study of Magnetic Manganites”, University of Oxford, 2012.
- [5] S.-W. Cheong and M. Mostovoy, *Nature Materials* 6, 13 (2007).
- [6] A. B. Sushkov, R. V. Aguilar, S. Park, S-W, Cheong and H. D. Drew, *Phys Rev Lett.* 98, 027202 (2007).
- [7] J. Varignon, S. Petit, A. Gellé, and M. B. Lepeitit, “*J Phys Condens Matter.*;25(49):496004”, 2013.
- [8] L. C. Chapon, P. G. Radaelli, G. R. Blake, S. Park, and S.-W. Cheong, *Phys. Rev. Lett.* 96, 097601 (2006).
- [9] A. RAMIREZ, *Geometrical Frustration*, chapter 4, p. 423, Elsevier Science B.V., 2001.
- [10] N. Hur, S. Park, P.A. Sharma, J. S. Ahn, S. Guha and S-W.Cheong, *Nature* 429, 392 (2004).
- [11] G. R. Blake, L. C. Chapon, P. G. Radaelli, S. Park, N. Hur, S-W. Cheong, and J. Rodríguez-Carvajal, *Phys. Rev. B* 71, 214402 (2005).
- [12] Tay-Rong Chang, Horng-Tay Jeng, Chung-Yuan Ren, and Chen-Shiung Hsue, *Phys. Rev. B* 84, 024421 (2011).
- [13] N. Hur, S. Park, P. A. Sharma, S. Guha, and S-W. Cheong, *Phys. Rev.Lett.* 93, 107207 (2004).
- [14] D. Tzankov, V. Skumryev, M. Aroyo, R. Puzniak, M.D. Kuz'min, M. Mikhov, *Solid.Stat. Comm.* 147, 212 (2008).
- [15] L. C. Chapon, G. R. Blake, M. J. Gutmann, S. Park, N. Hur, P. G. Radaelli, and S. W. Cheong, *Phys. Rev. Lett.*93, 177402 (2004).
- [16] I. A. Sergienko and E. Dagotto, *Phys. Rev. B.* 73, 094434 (2006).
- [17] A. Muñoz, J. A. Alonso, M. T. Casais, M. J. Martínez-Lope, J. L. Martínez, and M. T. Fernández-Díaz, *Phys. Rev. B* 65, (2002)144423
- [18] P. Blaha, K. Schwarz, G. Madsen, D. Kvasnicka, and J. Luitz, *WIEN 2k, Augmented Plane Wave Local Orbitals Program for Calculating Crystal Properties*, Vienna, Austria, 2001.
- [19] J. P. Perdew, K. Burke, and M. Ernzerhof, *Phys. Rev. Lett.* 77, 3865 (1996)
- [20] J. P. Perdew, K. Burke, M. Ernzerhof, *Generalized Gradient Approximation Made Simple*, *Phys. Rev. Lett.* , Vol. 77, No. 18, (1996).
- [21] L. Hedin, B. I. Lundqvist, *Explicit local exchange-correlation potentials*, *J. Phys. C: Solid St. Phys.* , Vol. 4, (1971).
- [22] S.Y. Savrasov and G. Kotliar. *Phys. Rev. Lett.*, 84, 3670 (2000).
- [23] B.-T. Wang, H. Shi, W. Li, and P. Zhang, *Phys. Rev. B* 81, 045119 (2010).

- [24] H. J. Monkhorst and J. D. Pack, Phys. Rev. B 13, 5188 (1976).
- [25] P. Carra, B. T. Thole, M. Altarelli and X. Wang, Phys. Rev. Lett., 70, 694, Feb. 1993.
- [26] L. C. Chapon, G. R. Blake, M. J. Gutmann, S. Park, N. Hur, P. G. Radaelli, and S.-W. Cheong, "Structural anomalies and multiferroic behavior in magnetically frustrated  $\text{TbMn}_2\text{O}_5$ ," Phys. Rev. Lett., vol. 93, p. 177402, Oct 2004.
- [27] P. G. Radaelli, C. Vecchini, L. C. Chapon, P. J. Brown, S. Park, and S.-W. Cheong, "Incommensurate magnetic structure of  $\text{YMn}_2\text{O}_5$  : A stringent test of the multiferroic mechanism," Physical Review B, vol. 79, p. 020404, jan 2009.
- [28] C. Tay-Rong, J.Horng-Tay, R. Chung-Yuan, H. Chen-Shiung, Phys Rev B,84.024421(2011).
- [29] B. T. Thole, P. Carra, F. Sette and G. van der Laan, Phys. Rev. Lett., 68, 1943 (1992).
- [30] C. Wilkinson, P. J. Brown, and T. Chatterji, Phys. Rev. B. 84, 224422 (2011).
- [31] M. Balli, S. Jandl, P. Fournier, D. Z. Dimitrov, Crystals 2017, 7, 44.
- [32] J. Jensen and A. R. Mackintosh, Rare Earth Magnetism (Oxford Univ. Press, Oxford, 1991)
- [33] H. Bouhani, A. ENDICHI et al, Journal of "Materials Chemistry and Physics", 10.1016/2019.04.044.
- [34] Chenjie Wang, Guang-Can Guo, and Lixin He, Materials Science, 2007, arXiv:0711.2539v1.
- [35] M. Balli, B. Roberge, P. Fournier, et S. Jandl, « Review of the Magnetocaloric Effect in  $\text{RMnO}_3$  and  $\text{RMn}_2\text{O}_5$  Multiferroic Crystals », *Crystals*, vol. 7, n° 2, p. 44, févr. 2017, doi: 10.3390/cryst7020044.